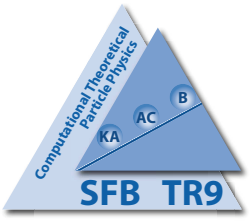

Massive Tadpoles: Techniques and Applications

Konstantin G. Chetyrkin[a], Johann H. Kühn[a], Matthias Steinhauser[a], Christian Sturm[b]

[a] *Institut für Theoretische Teilchenphysik, Karlsruher Institut für Technologie (KIT), Wolfgang-Gaede-Straße 1, D-76128 Karlsruhe, Germany*
[b] *Universität Würzburg, Institut für Theoretische Physik und Astrophysik, Emil-Hilb-Weg 22, D-97074 Würzburg, Germany*

Abstract

A brief discussion of massive tadpole diagrams and their phenomenological consequences is presented. This includes predictions of the ρ parameter and, as a consequence, the mass of the W boson, implications on the charm and bottom quark masses from the moments, i.e. the derivatives of the current correlators, and the Higgs boson decay rate. A fairly consistent picture emerges, with $m_c(3\text{ GeV}) = 0.986 \pm 0.013$ GeV and $m_b(m_b) = 3.610 \pm 0.016$ GeV. Furthermore, fairly stringent predictions for the Higgs decay rate into photons and gluons are obtained, which will be interesting in increasingly precise experiments.

Keywords: vacuum integrals, ρ parameter, charm and bottom quark mass, decoupling, Higgs production and decay

1. Introduction

Using massive tadpole diagrams significant progress has been made in the improved prediction of various physical quantities. They have, e.g., contributed to an amazingly precise relation between quark masses (in particular the top-quark mass M_t), the mass of the Higgs boson, M_H, and the masses of the gauge bosons, M_W and M_Z. Three- and even four-loop corrections have become accessible during the past years. Direct and indirect measurements are well consistent, at least within the current world average $M_t = 173.21 \pm 0.51 \pm 0.71$ GeV [1] and $M_H = 125.7 \pm 0.4$ GeV [1]. Current-current correlators, evaluated in three- and partially four-loop approximation are thus an indispensable tool for tests of the Standard Model (SM), as we will discuss in more detail in Section 2.

The evaluation of three- and even four-loop tadpole diagrams is directly related to the evaluation of moments of the charm- and bottom-quark correlators. These may in turn lead to a precise determination of charm- and bottom-quark masses. Since all these quantities, in turn, are directly accessible, both to a perturbative and a non-perturbative treatment, a remarkably consistent picture emerges. In fact the analysis for the charm- as well as the bottom-quark mass leads to $m_c(3\text{ GeV}) = 0.986 \pm 0.013$ GeV and $m_b(10\text{ GeV}) = 3.610 \pm 0.016$ GeV [2, 3], a result quite comparable to other methods, in particular to non-perturbative studies as will be discussed in Section 3.

Finally, in Section 4, we list a collection of topics and results which are connected to the main theme of this article. This includes the decoupling of heavy quarks at four loops, the Higgs-gluon coupling up to five-loop order, and the Higgs-decay rate into two photons at three and four loops, including non-singlet and singlet terms.

2. Weak corrections

Let us start with the ρ parameter, the quantity introduced in the early times of electroweak interactions of the SM. In its more modern version it gives the relation between gauge boson masses, the weak- and the electromagnetic coupling G_F and α, a relation, which exists at tree level already. In higher orders this relation depends on all remaining parameters of the SM. The radiative corrections are dominated by the quadratic dependence on the mass of the top quark M_t, the logarithmic dependence on the Higgs boson, M_H, and, to a lesser extent, also on the masses of the remaining quarks m_q and

leptons m_ℓ:

$$M_W = f(G_F, M_Z, \alpha; M_t, M_H; m_q, m_\ell). \quad (1)$$

A slightly different version of the same equation

$$M_W^2\left(1 - \frac{M_W^2}{M_Z^2}\right) = \frac{\pi\alpha}{\sqrt{2}G_F}(1 + \Delta r) \quad (2)$$

makes the presence of the electroweak corrections even more transparent. This equation can be rewritten and simplified even further by separating Δr into a piece which is dominated by weak effects and another one which is dominated by electromagnetic effects, mainly due to the running of the electromagnetic coupling $\Delta\alpha$ (see Refs. [4] and [5] for three- and four-loop corrections, respectively). Furthermore, it is convenient to separate the leading M_t^2 dependence which leads to

$$\Delta r = -\frac{\cos^2\theta_W}{\sin^2\theta_W}\Delta\rho + \Delta\alpha + \Delta r_{\text{remaining}}\,. \quad (3)$$

Here $\Delta\rho = 3G_F M_t^2/(8\sqrt{2}\pi^2)+\ldots$ incorporates the dominant weak terms evaluated in leading order by Veltman [6] nearly 40 years ago.

It is the aim of ongoing and of future theoretical studies to compete with the precision anticipated for the next round of experiments. The present precision and the precision anticipated for the future (as far as δM_W and δM_t are concerned) are given by

δM_W [MeV]	δM_t [GeV]	
33	5	status 2003 (LEP, TEV)
15	0.76	now (TEVATRON, LHC)
8→5	0.6	aim (LHC); theory
3→1.2	0.1-0.2	ILC, TLEP

As it turns out, the relative shifts of M_W and M_t are just of the right order of magnitude to explore the sensitivity towards radiative corrections. This is seen most clearly by considering the shift in M_t that is compensated by a shift in M_W

$$\delta M_W \approx 6\cdot 10^{-3}\delta M_t\,, \quad (4)$$

keeping $\alpha(M_Z)$, M_Z and M_H fixed.

Let us now recall the development of the theory predictions for $\Delta\rho$ during the past one or two decades.

Early results related to the two-loop approximation can be found in Refs. [7, 8]. These papers are based on the approximation $M_t^2 \gg M_W^2$. The first step into the three-loop regime was taken in the limit $M_H = 0$ [9]. In fact, this turns out to be a poor approximation, leading to tiny corrections for the terms of order X_t^3 and $\alpha_s X_t^2$ with

$$X_t = \frac{G_F M_t^2}{8\sqrt{2}\pi^2}\,. \quad (5)$$

The first three-loop result with M_H different from zero requires the full set of three-loop tadpoles [10]. At order $\alpha_s X_t^2 f(M_t/M_H)$ this corresponds to QCD corrections to the two-loop diagrams of order $X_t^2 f(M_t/M_H)$ (see Fig. 1 for a sample Feynman diagram). At order $X_t^3 f(M_t/M_H)$ diagrams with one quark line contribute, as well as those involving two disconnected quark lines.

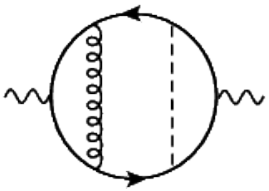

Figure 1: Sample diagram for the $\alpha_s X_t^2 f(M_t/M_H)$ contribution. Solid lines denote top quarks, dashed lines Higgs or Goldstone bosons and curly lines gluons.

At the same time the translation from the $\overline{\text{MS}}$ mass $m_t(M_t)$ to the pole mass M_t has to be performed at two loops. This corresponds to the evaluation of two-loop on-shell diagrams. For the case of the $X_t^3 f(M_t/M_H)$ corrections the counterterms are of order X_t^2 and are depicted in Fig. 2.

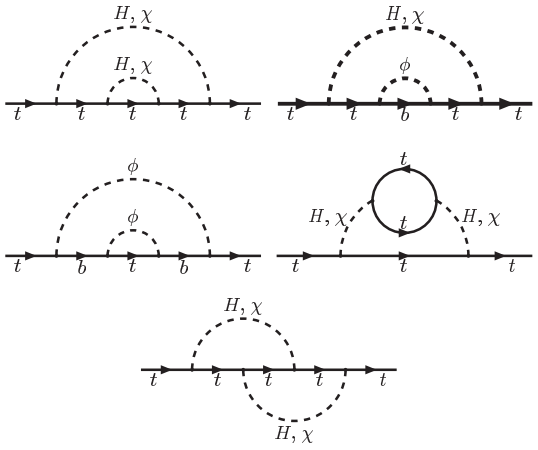

Figure 2: Two-loop on-shell diagrams which contribute to the translation of the $\overline{\text{MS}}$ mass to the pole mass.

In contrast to the pure QCD problem (see Section 3) with only one mass scale being present (and which can therefore be expressed in closed analytic form) here one typically encounters two different scales, M_H and M_t. A closed analytical solution is no longer at hand. There are, however, various cases which allow for expansions, one of which is perfectly valid for M_H and M_t in the region of interest. Analytic results are available in the cases $M_H = 0$ and $M_H = M_t$, where only one scale is present. Expansions, which in principle allow

for arbitrary high precision are then accessible in two cases: for the case of large M_H with the approximation in $(M_t^2/M_H^2)^n$ modulo logarithms which is valid down to $M_H \approx 2M_t$ and the case of M_H around M_t which is valid from fairly small M_H, say $M_H \approx 0.1M_t$, up to $M_H \approx 2M_t$. The results for the expansion in $(M_H/M_t)^n$ and in $(M_H - M_t)^2/M_t^2$ are shown in Fig. 3. Note that for $M_H = 0/126$ GeV one obtains for the prefactor of $\alpha_s X_t^2$, a part of the three-loop term of $\Delta\rho$, the values 2.9/120.

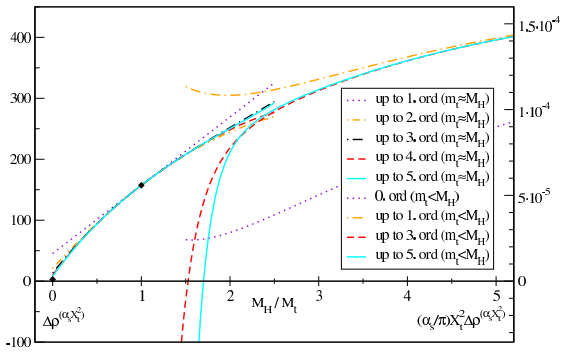

Figure 3: Contributions of order $\alpha_s X_t^2$ to $\Delta\rho$ in the on-shell definition of the top-quark mass. The black squares indicate the points where the exact result is known. Using the latest numerical values for M_t and M_H one obtains $M_H/M_t \approx 0.73$.

The results for the shift in M_W and the effective weak mixing angle are shown in Fig. 4 for the four contributions which are most relevant. The terms proportional to X_t and $X_t\alpha_s$ must be taken into account in any sensible analysis and amount to a shift in $\delta\rho$ of order 0.00865.

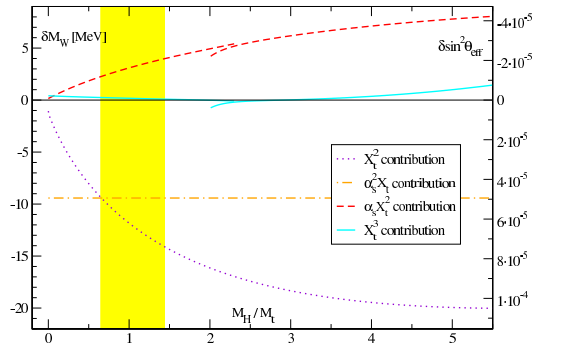

Figure 4: The shift in M_W and $\sin^2\theta_{\rm eff}$ as a function of M_H/M_t induced by the corrections of order X_t^2, $\alpha_s^2 X_t$, $\alpha_s X_t^2$, and X_t^3.

The two-loop piece proportional to X_t^2 is of the same order as the three loop piece, proportional to $\alpha_s^2 X_t$. The purely weak term proportional X_t^3 is negligible now and in the foreseeable future, the term proportional to $\alpha_s X_t^2$ is just below the present sensitivity.

Four-loop QCD contributions

Two- and three-loop QCD corrections to $\Delta\rho$ have been computed in Refs. [11–16] about 20 years ago. As stated above, since several years it is now possible to push the predictions for the ρ parameter to the four-loop level. This requires, on the one hand, the relation between pole- and $\overline{\rm MS}$ mass in three-loop approximation [17, 18] and, on the other hand, the evaluation of about fifty four-loop tadpole diagrams. This has been achieved by a combination of analytically methods, difference equations and semi-numerical integration [19–21]. In a first step this has lead to the four-loop result for the ρ parameter in the $\overline{\rm MS}$ scheme

$$\delta\rho_t^{(4\,\rm loops)} = 3\frac{G_F\overline{m}_t^2}{8\sqrt{2}\pi^2}\left(\frac{\alpha_s}{\pi}\right)^3 \underbrace{(-3.2866 + 1.6067)}_{-1.6799} . \quad (6)$$

The first term has been evaluated in Ref. [22], the second one, which (in the $\overline{\rm MS}$ scheme) leads to a reduction by a factor of about 1/2, in Refs. [19, 20]. For the numerical evaluation the translation from the $\overline{\rm MS}$ to the pole mass is more convenient and one finds

$$\delta\rho_t^{(4\,\rm loops)} = 3\frac{G_F M_t^2}{8\sqrt{2}\pi^2}\left(\frac{\alpha_s}{\pi}\right)^3 (-93.1501) \quad (7)$$

which corresponds to a shift in M_W by about 2 MeV, similar to the three loop term of order $\alpha_s X_t^2$.

3. Charm- and bottom-quark masses

The precise determination of the charm- and bottom-quark masses from relativistic four-loop moments can be considered as one of the truly remarkable successes of quantum field theory with remarkable agreement between perturbative [2, 3] and lattice methods [23–25]. Let us first give a more detailed motivation, then present the theoretical framework and finally compare the results based on perturbative and lattice methods.

Precise bottom quark masses enter many B physics quantities. During the past years significant progress has been made on the one hand in the analysis of B-meson decays and, on the other hand, the Υ spectroscopy. In particular the latter has led to a fairly consistent result of $m_b(m_b) = 4.193^{+0.022}_{-0.035}$ GeV [26] (see also Ref. [27] where $m_b(m_b) = 4.169 \pm 0.009$ GeV has been

obtained) in excellent agreement with the result based on sum rules discussed in detail below.

Let us further motivate the need for precise quark masses for the case of the bottom-quark mass, which enters a number of physical observables. Most prominently, we want to mention the decay of a Higgs boson into bottom quarks which, using the scalar correlator to five-loop precision [28], can be written in the form

$$\begin{aligned}\Gamma(H\to b\bar{b}) &= \frac{G_F M_H^2}{4\sqrt{2}\pi} m_b^2(M_H) R^{(S)}(M_H) \qquad (8)\\ R^{(S)}(M_H) &= 1 + 5.667\left(\frac{\alpha_s}{\pi}\right) + 29.147\left(\frac{\alpha_s}{\pi}\right)^2 \\ &\quad + 41.758\left(\frac{\alpha_s}{\pi}\right)^3 - 825.7\left(\frac{\alpha_s}{\pi}\right)^4 \\ &= 1 + 0.19551 + 0.03469 \\ &\quad + 0.00171 - 0.00117. \qquad (9)\end{aligned}$$

The theory uncertainty, which is generously taken from a variation of the scale parameter between $M_H/3$ and $3M_H$, is reduced from 5‰ for the four-loop to 1.5‰ for the five-loop result. Thus, the main uncertainty is induced from the uncertainty of the bottom quark mass which (at energy scale 10 GeV) is given by [3]

$$m_b(10\ \text{GeV}) = \left(3610 - \frac{\alpha_s - 0.1189}{0.002}\cdot 12 \pm 11\right)\ \text{MeV}\,.$$

The running from 10 GeV to M_H depends on the anomalous mass dimension γ_m, the β function and on α_s. With the present knowledge (i.e. four-loop anomalous dimensions as implemented in `RunDec` [29, 30]) one finds

$$m_b(M_H) = 2759 \pm 8|_{m_b} \pm 27|_{\alpha_s}\ \text{MeV}\,. \qquad (10)$$

It is interesting to investigate the effect of the five-loop anomalous dimensions. Taking into account the γ_m to five-loop accuracy [31, 32] together with β_4, the five-loop contribution to the β function of QCD, which is still unknown, one obtains the following uncertainties

$$\begin{aligned}\frac{\delta m_b^2(M_H)}{m_b^2(M_H)} &= -1.3\times 10^{-4}(\beta_4/\beta_0 = 0)\\ &= -4.3\times 10^{-4}(\beta_4/\beta_0 = 100)\\ &= -7.3\times 10^{-4}(\beta_4/\beta_0 = 200)\,, \qquad (11)\end{aligned}$$

which lead to an uncertainty of a few MeV in $m_b(M_H)$ which is small compared to the current error shown in Eq. (10).

Another motivation which also points to a precision around 10 MeV is based on the picture of Yukawa unification. In this approach $\lambda_\tau \sim \lambda_b \sim \lambda_t$ at the GUT scale. In effect this implies $\delta m_b/m_b \sim \delta m_t/m_t$. Assuming a precision of the top-quark mass $\delta m_t \approx 0.5$ GeV then leads to a precision of $\delta m_b \approx 10$ MeV, consistent with our finding below.

SVZ sum rules, moments and tadpoles

The main idea originally advocated in Ref. [33] is based on the observation (cf. Fig. 5), that the cross section for hidden (J/Ψ plus $\Psi(2S)$) plus open ($D\overline{D}$ plus resonances) charm production is well described by perturbation theory, if the analysis is restricted to sufficiently low moments.

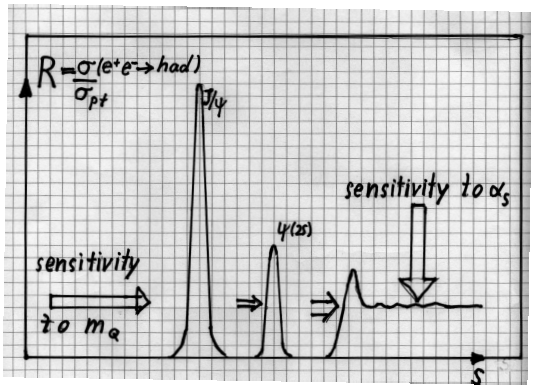

Figure 5: Sketch of the R ratio in the charm-threshold region.

Let us first recall some definitions. The two-point correlation function

$$(-q^2 g_{\mu\nu} + q_\mu q_\nu)\Pi(q^2) = \mathrm{i}\int dx e^{iqx}\langle 0|T\, j_\mu(x) j_\nu(0)|0\rangle$$

is related to the electromagnetic current j_μ as follows

$$R(s) = 12\pi \mathrm{Im}\left[\Pi(q^2 = s + \mathrm{i}\varepsilon)\right]\,. \qquad (12)$$

In fact, we are only interested in lowest moments of Π, corresponding to the first few terms of the Taylor expansion of $\Pi(q^2)$:

$$\Pi(q^2) = Q_q^2 \frac{3}{16\pi^2}\sum_{n\geq 0}\overline{C}_n z^n\,, \qquad (13)$$

where Q_q corresponds to the charge of the considered quark. Here $z = q^2/(4m_q^2)$ and $m_q = m_q(\mu = m_q)$ is the $\overline{\rm MS}$ mass at the scale $\mu = m_q$. Let us, for definiteness, restrict the following discussion to the charm quark, i.e., $q = c$.

For the moments one finds

$$\begin{aligned}\overline{C}_n &= \overline{C}_n^{(0)} + \frac{\alpha_s}{\pi}\overline{C}_n^{(1)} + \left(\frac{\alpha_s}{\pi}\right)^2\overline{C}_n^{(2)}\\ &\quad + \left(\frac{\alpha_s}{\pi}\right)^3\overline{C}_n^{(3)} + \ldots\,, \qquad (14)\end{aligned}$$

if the renormalization scale is set to $\mu = m_q$ or

$$\begin{aligned}\overline{C}_n &= \overline{C}_n^{(0)} + \frac{\alpha_s}{\pi}\left(\overline{C}_n^{(10)} + \overline{C}_n^{(11)} l_{m_c}\right) \\ &+ \left(\frac{\alpha_s}{\pi}\right)^2 \left(\overline{C}_n^{(20)} + \overline{C}_n^{(21)} l_{m_c} + \overline{C}_n^{(22)} l_{m_c}^2\right) \\ &+ \left(\frac{\alpha_s}{\pi}\right)^3 \left(\overline{C}_n^{(30)} + \overline{C}_n^{(31)} l_{m_c} + \overline{C}_n^{(32)} l_{m_c}^2 \right. \\ &\left. + \overline{C}_n^{(33)} l_{m_c}^3\right) + \ldots, \end{aligned} \tag{15}$$

if one is interested in the generic form with $l_{m_c} = \ln(m_c^2(\mu)/\mu^2)$. The next-to-next-to-leading order calculation had been performed already nearly twenty years ago [34–36] and is available for all four (vector, axial, scalar and pseudoscalar) correlators. The original evaluation was up to $n = 8$. More recently, this has been extended to $n = 30$ [37, 38]. Now this project has been pushed to N^{3}LO, and the results will be described in the following. In a first step the n_f^2 contribution has been computed for $\overline{C}_0$ and $\overline{C}_1$ [39], then the complete result became available. The reduction of the many different diagrams has been performed to 13 master integrals, shown in Fig. 6, using the Laporta algorithm [40]. Subsequently these 13 remaining integrals are evaluated, using originally a combination of numerical and analytical, now purely analytical methods.

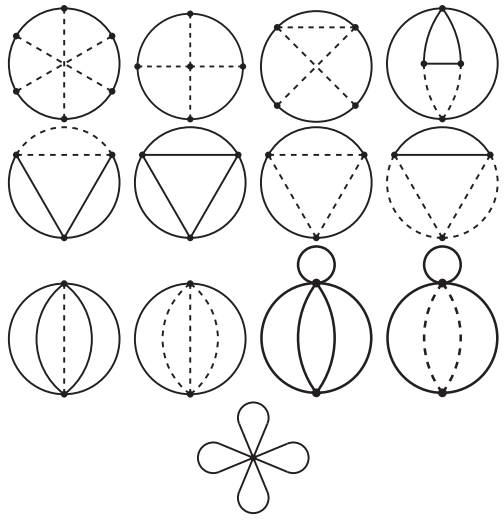

Figure 6: The 13 master integrals. Solid lines denote massive propagators; dashed lines represent massless propagators.

The reduction of hundreds of integrals to master integrals has been achieved, originally for $\overline{C}_0$ and $\overline{C}_1$ [41, 42], subsequently for $\overline{C}_2$ and $\overline{C}_3$, using the program Crusher [43, 44]. In the meantime all master integrals are known in closed analytic form to high order in ε, using results by a number of different authors (see Refs. [45–48] and references therein). The results for $\overline{C}_4$ up to $\overline{C}_{10}$ are known approximately, using an approximation based on additional information from low energies ($q^2 = 0$), from threshold ($q^2 = 4m^2$) and from high energy [49–51]. Closely related results are also known for axial, scalar and pseudoscalar correlators [44, 50, 52]. These can be used for the investigation of correlators on the lattice [23] and will not be investigated further in this more phenomenological study. The heavy quark vector current correlator for $q^2 \ll m^2$ has also been determined in the large β_0 limit [53] in order to study the large-order behaviour.

n	$\mathcal{M}_n^{\rm res}$ $\times 10^{(n-1)}$	$\mathcal{M}_n^{\rm thresh}$ $\times 10^{(n-1)}$	$\mathcal{M}_n^{\rm cont}$ $\times 10^{(n-1)}$	$\mathcal{M}_n^{\rm exp}$ $\times 10^{(n-1)}$	$\mathcal{M}_n^{\rm np}$ $\times 10^{(n-1)}$
1	0.1201(25)	0.0318(15)	0.0646(11)	0.2166(31)	−0.0001(2)
2	0.1176(25)	0.0178(8)	0.0144(3)	0.1497(27)	0.0000(0)
3	0.1169(26)	0.0101(5)	0.0042(1)	0.1312(27)	0.0007(14)
4	0.1177(27)	0.0058(3)	0.0014(0)	0.1249(27)	0.0027(54)

Table 1: The experimental moments in $(\text{GeV})^{-2n}$ as defined in Eq. (18) are shown, separated according to the contributions from the narrow resonances, the charm threshold region and the continuum region above $\sqrt{s} = 4.8$ GeV. The last column gives the contribution from the gluon condensate.

The moments are directly related to measurements as follows. From theoretical considerations one finds

$$\begin{aligned}\mathcal{M}_n^{\rm th} &\equiv \frac{12\pi^2}{n!}\left(\frac{d}{dq^2}\right)^n \Pi_c(q^2)\Big|_{q^2=0} \\ &= \frac{9}{4}Q_c^2\left(\frac{1}{4m_c^2}\right)^n \overline{C}_n\,, \end{aligned} \tag{16}$$

where the quantity $\overline{C}_n$ depends on $\alpha_s(\mu^2)$ and $\ln(m_c^2/\mu^2)$. As default value for μ we use $\mu = 3$ GeV.

To obtain experimental moments one considers the correlator given by

$$\Pi_c(q^2) = \frac{q^2}{12\pi^2}\int \mathrm{d}s \frac{R_c(s)}{s(s-q^2)} + \text{subtraction}\,, \tag{17}$$

which leads to

$$\mathcal{M}_n^{\rm exp} = \int \frac{\mathrm{d}s}{s^{n+1}} R_c(s)\,. \tag{18}$$

Imposing the constraint $\mathcal{M}_n^{\rm exp} = \mathcal{M}_n^{\rm th}$ leads to m_c at the scale $\mu = 3$ GeV, a result that could be easily translated to arbitrary values of μ.

Let us first discuss the ingredients for charm, and then for bottom quarks. The results for the electronic widths of J/Ψ and Ψ' are taken from the combination of BES, CLEO and BABAR experiments, and for the continuum $R(s)$ from BES. For the charm case there is also a non-perturbative contribution which is, however,

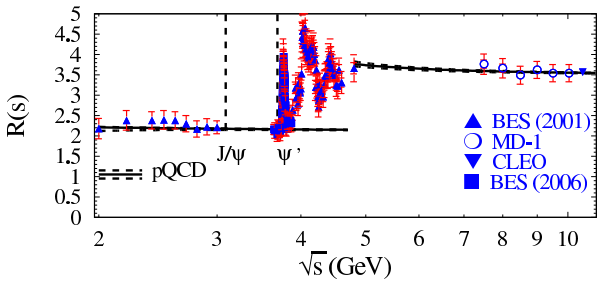

Figure 7: The normalized cross section $R(s)$ between 2 GeV and 10 GeV. The solid line corresponds to the theoretical prediction. The uncertainties obtained from the variation of the input parameters and of μ are indicated by the dashed curves. The inner and outer error bars give the statistical and systematical uncertainty, respectively. The data points are from BES [54, 55], MD-1 [56] and CLEO [57]. The vertical dashed lines correspond to the location of the J/Ψ and Ψ' resonances.

negligible for the three lowest moments and remains relatively small even for the fourth. A careful investigation of non-perturbative terms combined with the extrapolation of R_{uds} as well as R_c in the region sufficiently far above the respective threshold leads to a remarkably consistent result, with errors on $m_c(3\text{ GeV})$, as extracted for $n = 1$ to 3, below 20 MeV. The result for the moments individually split into contributions from the narrow resonances, threshold and continuum region is shown in Tab. 1. $R(s)$ around the charm threshold region is shown in Fig 7.

In particular we observe a remarkable consistency between the results for $n = 1, 2, 3$ and 4 and a relatively small shift when moving from three- to four-loop approximation (cf. Fig. 8).

n	$m_c(3\text{ GeV})$	exp	α_s	μ	np	total
1	986	9	9	2	1	13
2	976	6	14	5	0	16
3	978	5	15	7	2	17
4	1004	3	9	31	7	33

Table 2: The second column shows the results for $m_c(3\text{ GeV})$ in MeV. The errors in the four inner columns are from experiment, α_s, variation of μ and the gluon condensate. The last column shows the total error.

In taking the lowest moment as our final result we find [3]

$$m_c(3\text{ GeV}) = 986 \pm 13\text{ MeV}. \qquad (19)$$

When converted from $\mu = 3$ GeV to the scale m_c, this is modified to $m_c(m_c) = 1279 \pm 13$ MeV, nicely consistent with other determinations [23, 24]. The robustness of our result is demonstrated in Fig. 8, where the results are compared for different orders $O(\alpha_s^i)$, with i=0, 1, 2 and 3 and for different moments, with n varying between $n = 1$ and $n = 4$.

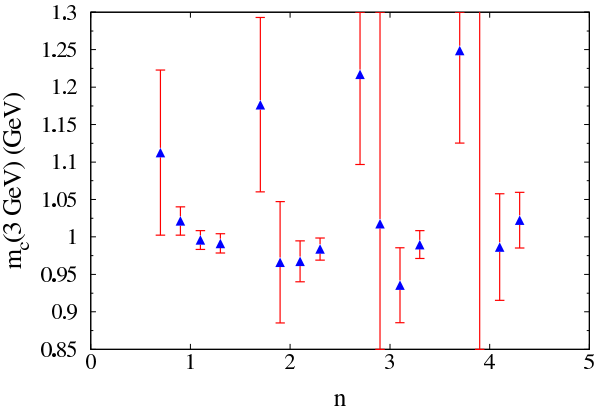

Figure 8: Dependence of $m_c(3\text{ GeV})$ on the number of moments n and on $O\left(\alpha_s^i\right)$ for $i = 0, \ldots, 3$.

The result can be compared to those from a large number of results, which are based on various different observables. Fig 9 shows a compilation of recent analyses [1–3, 23, 58–66].

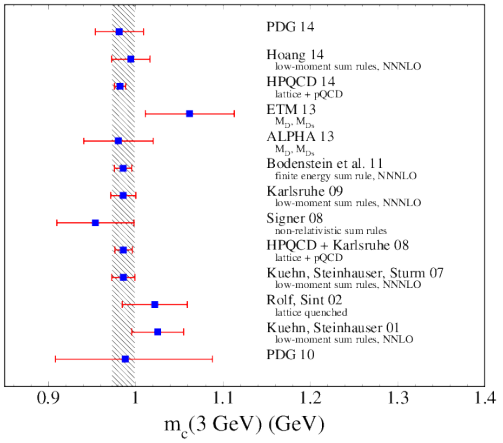

Figure 9: Comparison of $m_c(3\text{ GeV})$ with several other results.

Similar considerations are applicable for the corresponding investigations of the Υ-resonances and the mass of the bottom quark. For convenience of the reader we again list in Tab. 3 separately the contributions from the narrow resonances ($\Upsilon(1S) - \Upsilon(4S)$) [67], the threshold region (10.618 GeV-11.2 GeV) [68] and the perturbative continuum ($E > 11.2$ GeV).

For the lowest moment the latter gives the main contribution, starting from the second moment the resonance and the threshold regions are again dominant. In particular moments number two and three offer a fair

n	$\mathcal{M}_n^{\text{res,(1S-4S)}}$ $\times 10^{(2n+1)}$	$\mathcal{M}_n^{\text{thresh}}$ $\times 10^{(2n+1)}$	$\mathcal{M}_n^{\text{cont}}$ $\times 10^{(2n+1)}$	$\mathcal{M}_n^{\text{exp}}$ $\times 10^{(2n+1)}$
1	1.394(23)	0.287(12)	2.911(18)	4.592(31)
2	1.459(23)	0.240(10)	1.173(11)	2.872(28)
3	1.538(24)	0.200(8)	0.624(7)	2.362(26)
4	1.630(25)	0.168(7)	0.372(5)	2.170(26)

Table 3: Moments for the bottom quark system in $(\text{GeV})^{-2n}$

compromise between smallness of the error and the contribution of the threshold region. Significant progress has been made between the first measurements of CLEO [69] and the more recent one by the BABAR collaboration in particular in the continuum region. As expected [2] the original CLEO result is too large by a factor around 1.3 but reproduces well the qualitative behaviour. The more recent BABAR result [68], however, is significantly more precise and well in agreement with the expectations for the continuum, based on the parton cross section. Let us note in this connection that the original BABAR result for $R_b(s)$ has to be deconvoluted with respect to initial state radiation (ISR), a fact that leads to a slight shift of $R_b(s)$.

The results for the bottom quark mass for the lowest four moments are given in Tab. 4 [3, 61]. For our final results we choose $n = 2$ which leads to

$$\begin{aligned} m_b(m_b) &= 4.163 \pm 0.016 \text{ GeV}, \\ m_b(10\text{ GeV}) &= 3.610 \pm 0.016 \text{ GeV}, \\ m_b(M_H) &= 2.759 \pm 0.028 \text{ GeV}. \end{aligned} \tag{20}$$

n	$m_b(10\text{ GeV})$	exp	α_s	μ	total	$m_b(m_b)$
1	3597	14	7	2	16	4151
2	3610	10	12	3	16	4163
3	3619	8	14	6	18	4172
4	3631	6	15	20	26	4183

Table 4: The different columns show the results for $m_b(10\text{ GeV})$ in the second column, obtained from the different moments listed in the first column. The last column gives the value of $m_b(m_b)$. The three inner columns give the uncertainty due to the error in the experimental moments (exp), the uncertainty due to the error in α_s and the uncertainty due to the residual scale dependence μ. The second to last column gives the total uncertainty. All masses and uncertainties are in units of MeV.

The consistency, when comparing the results for the lowest four moments is very close to the one from 2007 [2], where only estimates were available for the four-loop term of $n = 2, 3$ and 4. Furthermore, only recalibrated results for the continuum corresponding to the aforementioned factor 1.3 were available. The result for $m_b(m_b)$ can also be compared to those from other studies in Fig. 10 [1–3, 24–27, 58, 61, 65, 70–72]. Although somewhat towards the low side, the result are well compatible with those of earlier investigations.

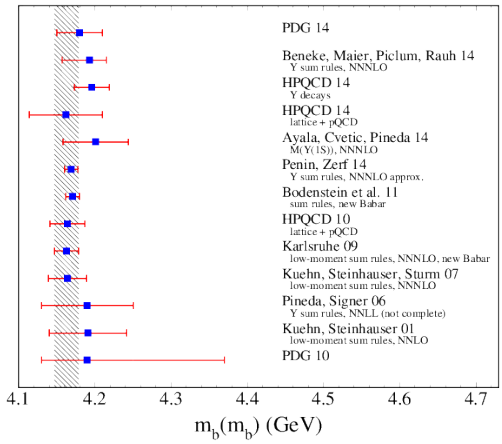

Figure 10: Comparison of $m_b(m_b)$ with several other determinations.

In Fig. 11 the results for the charm and bottom quark masses as obtained from the low-moment sum rules [2, 3, 58, 61] are compared with the numerical values proposed by the PDG for the years between 2000 and 2014. It is interesting to note that the extracted mass values, which were first based on three, later on four-loop perturbative input, remained rather constant whereas the PDG numbers seem to converge towards these results.

4. Further applications of massive tadpoles

Decoupling function at four loops

In many QCD applications the mass of a heavy quark m is much larger than the characteristic momentum scale $\sqrt{s}$ of a considered physical process. As a result these different mass scales involved in the process can lead to potentially large logarithms like $\log(\mu/\sqrt{s})$ or $\log(\mu/m)$ when using an MS-like renormalization scheme. In such a situation one can not set the renormalization scale μ to two different mass scales simultaneously, so that a proper choice of μ in order to avoid large logarithms is not possible anymore. However, by "integrating out" the heavy quark field one can construct an effective field theory with $n_l = n_f - 1$ light quarks only, where n_f is the number of quark flavours.

The $\overline{\text{MS}}$ coupling constants $\alpha_s^{(n_f)}$ and $\alpha_s^{(n_l)}$ of the quark-gluon interaction in the full n_f-flavor QCD and the effective n_l-flavor one are different and are related

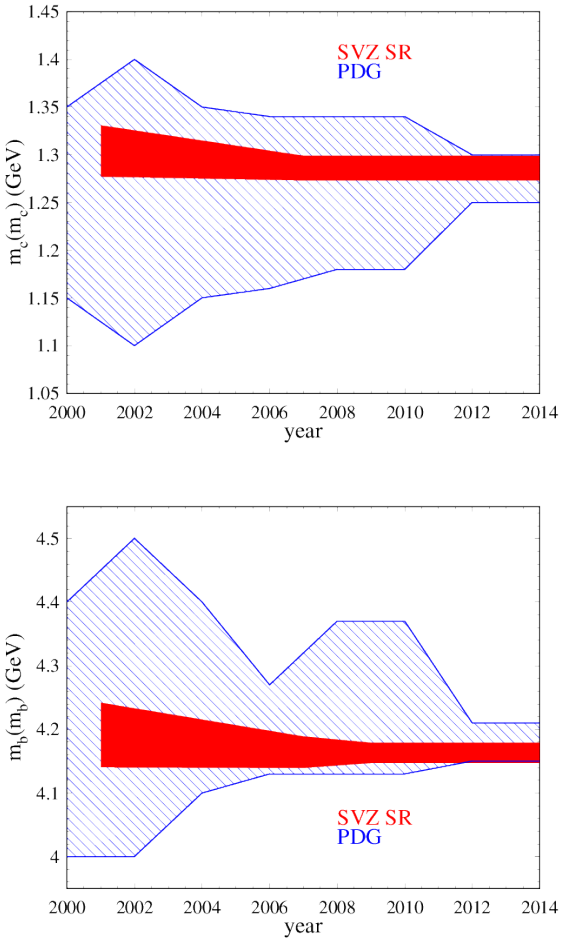

Figure 11: Comparison of $m_c(m_c)$ and $m_b(m_b)$ as obtained using low-moment sum rules [2, 3, 58, 61] (narrow band) and the values from the PDG between 2000 and 2014.

by the decoupling function $\zeta_g(\mu, \alpha_s^{(n_f)}(\mu), m)$ through the matching condition

$$\alpha_s^{(n_l)}(\mu) = \zeta_g^2(\mu, \alpha_s^{(n_f)}(\mu), m)\ \alpha_s^{(n_f)}(\mu). \tag{21}$$

At leading order the decoupling function is equal to one, but receives corrections in higher orders of perturbation theory. This matching condition for the $\overline{\rm MS}$ strong coupling constant α_s at a heavy quark threshold has been computed in Refs. [73, 74] to four-loop order. The decoupling function can be determined through the computation of polarization functions. The bare relation for ζ_g^0 reads [75]

$$\zeta_g^0 = \frac{\tilde{\zeta}_1^0}{\tilde{\zeta}_3^0 \sqrt{\zeta_3^0}}, \tag{22}$$

where

$$\begin{aligned} \zeta_3^0 &= 1 + \Pi_G^{0h}(0), \\ \tilde{\zeta}_3^0 &= 1 + \Pi_c^{0h}(0), \\ \tilde{\zeta}_1^0 &= 1 + \Gamma_{G\bar{c}c}^{0h}(0,0) \end{aligned} \tag{23}$$

with the gluon G and ghost c vacuum polarization functions $\Pi_G^{0h}(q^2)$ and $\Pi_c^{0h}(q^2)$. The vertex function $\Gamma_{G\bar{c}c}^{0h}(p,k)$ is the one-particle irreducible part of the amputated Green's function, where p and k are the outgoing four momenta of the fields c and G, respectively. The computation of these functions leads again to the evaluation of tadpole diagrams up to four-loop order. The four-loop contribution can be expressed in terms of the 13 master integrals shown in Fig. 6. The renormalized decoupling function is obtained from

$$\alpha_s^{(n_l)} = \left(\frac{Z_g^{(n_f)}}{Z_g^{(n_l)}}\zeta_g^0\right)^2 \alpha_s^{(n_f)}(\mu) \equiv \zeta_g^2 \alpha_s^{(n_f)}(\mu), \tag{24}$$

where $(Z_g)^2$ is the renormalization constant of the strong coupling constant.

The decoupling function plays an important role in testing QCD by running the strong coupling to different energy scales. For example, the strong coupling $\alpha_s(m_\tau)$ can be measured at the scale of the τ-lepton mass m_τ. In the next step one can run this value to the scale of the Z-boson mass M_Z by using the proper running and decoupling at the heavy charm- and bottom-quark thresholds and compare it to the experimentally measured result of $\alpha_s(M_Z)$. This procedure provides thus an excellent test of QCD asymptotic freedom. The four-loop contribution to the decoupling function leads to a reduction of the matching-related uncertainties in the evolution of $\alpha_s(m_\tau)$ to $\alpha_s(M_Z)$ by a factor of two [73, 74].

Higgs-gluon coupling to N⁴LO

Gluon fusion is the dominant production mechanism of the SM Higgs boson H at the Large Hadron Collider (LHC), where the leading order process is already at the one-loop level and the Higgs boson is produced by the fusion of two gluons through a heavy top-quark loop. The decoupling function enters in this context as an important building block since it can be used to derive the effective coupling of the Higgs boson to gluons via the following low-energy theorem

$$C_1^0 = -\frac{1}{2} m_t^0 \frac{\partial \ln \zeta_g^0}{\partial m_t^0}\,. \tag{25}$$

C_1 enters into an effective Lagrangian

$$\mathcal{L}_{\rm eff} = -2^{1/4} G_F^{1/2} H C_1 [O_1'] \tag{26}$$

in QCD with five flavours, where the top mass dependence is contained in C_1. The symbol G_F is the Fermi constant, and $[O'_1]$ is the renormalized form of the operator $O'_1 = G^{0'}_{a\mu\nu} G^{0'\mu\nu}_a$, where $G^{0'}_{a\mu\nu}$ is the gluon field strength tensor. The prime indicates that the object is in the effective five-flavour theory and the superscript 0 denotes a bare quantity. Using the four-loop result for ζ_g^2 of Refs. [73, 74] allows to determine C_1 in four-loop approximation, which confirms the result of Ref. [75] in a completely different and independent way. With the help of the anomalous dimensions even the five-loop contribution to C_1 has been predicted [73, 74] up to unknown five-loop n_f-dependent terms of the β function.

Decoupling of heavy quarks for the running of the fine structure constant

In complete analogy one can determine from the massive photon vacuum polarization function the photon decoupling function $\left(\zeta^0_{g\gamma}\right)^2$

$$\left(\zeta^0_{g\gamma}\right)^2 = \frac{1}{1 + \Pi^{0h}_\gamma(0)}\,. \tag{27}$$

The three-loop results of Ref. [75] have been extended to four loops in Ref. [76]. Starting from three-loop order there arise also diagrams where the external photon couples to massless fermions with the insertion of a heavy fermion loop. At four-loop order also singlet type diagrams arise for the first time, where the photon couples to two different fermion loops. Some example diagrams are shown in Fig. 12.

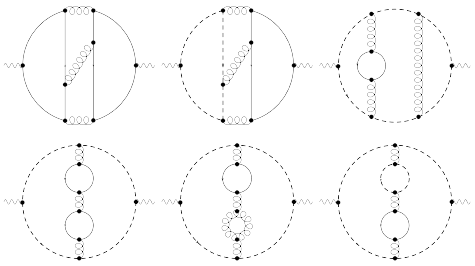

Figure 12: The first two diagrams are example singlet diagrams; the last four diagrams are examples for the situation where the external photon couples to a massless fermion loop with the insertion of a heavy internal fermion loop. The solid lines represent heavy top-quarks, the twisted lines denote gluons, and the dashed lines represent massless quarks.

Higgs boson decay to photons

The photon decoupling function can be used to determine higher order QCD corrections to the partial decay width of the Higgs boson into two photons (γ). The amplitude of the partial decay width $H \to \gamma\gamma$

$$\Gamma(H \to \gamma\gamma) = \frac{M_H^3}{64\pi}\left|A_W(\tau_W) + \sum_f A_f(\tau_f)\right|^2, \tag{28}$$

consists of two parts, a purely bosonic part $A_W(\tau_W)$ and a purely fermionic part $A_f(\tau_f)$ with $\tau_W = M_H^2/(4M_W^2)$ and $\tau_f = M_H^2/(4M_f^2)$. Higher order QCD corrections modify the fermionic part $A_f(\tau_f)$ of the amplitude. The top quark gives a dominant contribution to the amplitude A_f ($f = t$), since it is the heaviest fermion in the SM. In the heavy top-quark mass limit one can again describe the Higgs-photon-photon interaction in terms of an effective Lagrangian approach

$$\mathcal{L}_{\rm eff} = -\frac{H^0}{v^0}\, C^0_{1\gamma}\, F'^{0,\mu\nu} F'^0_{\mu\nu}\,, \tag{29}$$

with the vacuum expectation value v^0 and the field strength tensor $F'^0_{\mu\nu}$. The subscript 0 indicates a bare quantity and the prime denotes that the quantity is considered in the effective theory with n_l light active quark flavours. The coefficient function $C^0_{1\gamma}$ depends on the photon decoupling function

$$C^0_{1\gamma} = -\frac{1}{2} m_t^0 \frac{\partial \ln \zeta^0_{g\gamma}}{\partial m_t^0}. \tag{30}$$

This approach allows one to determine the leading contributions in the heavy top-quark mass limit to the Higgs-boson decay into two photons, where the external photons couple to the same heavy fermion loop, the so called non-singlet contributions.

At three-loop order in perturbative QCD the non-singlet contributions to the decay $H \to \gamma\gamma$ have been computed in Ref. [77] with several different methods, including power corrections of the order $[M_H^2/(4M_t^2)]^2$. The singlet contributions have been added in Ref. [78], where also additional power corrections of higher orders in $M_H^2/(4M_t^2)$ were calculated. The singlet contributions appear for the first time at three-loop order. An example diagram is shown in Fig. 13.

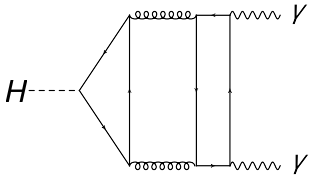

Figure 13: Example three-loop singlet diagram. Solid lines denote top quarks, wavy lines are photons, twisted lines represent gluons and the dashed line is the Higgs boson.

In Ref. [75] $C_{1\gamma}$ has been determined at four-loop order in the effective Lagrangian approach with the help of the knowledge of the anomalous dimensions. This result was subsequently also obtained independently through the calculation of the four-loop order of the decoupling function $\zeta_{g\gamma}$ in Ref. [76], where also the corresponding five-loop contributions were determined, with the help of the anomalous dimensions. Some example diagrams at four-loop order are depicted in Fig. 14.

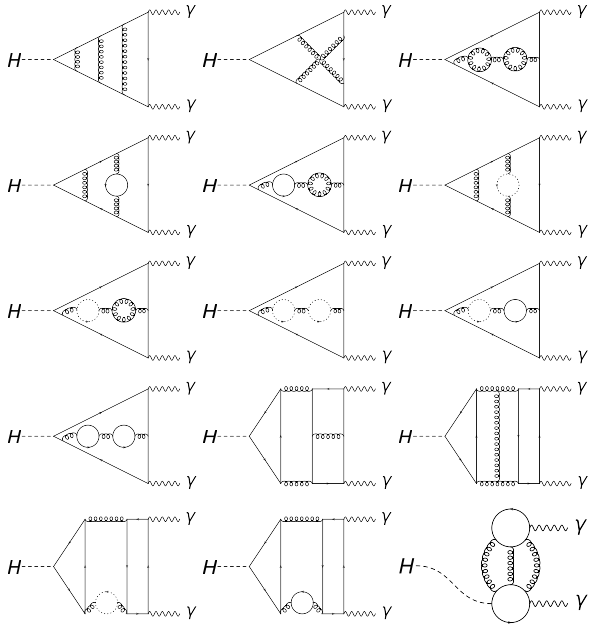

Figure 14: Example diagrams which illustrate different kind of diagram classes which have been determined in the heavy top-quark mass limit at four-loop order. Dotted lines represent massless quarks; all other lines are as defined in Fig. 13.

5. Conclusions

The systematic investigation of four-loop tadpole integrals started about a decade ago. In this article we have briefly touched the techniques which have been developed to perform the reduction to master integrals and to obtain results for the latter. Furthermore, we have described in some detail the most important applications. Among them are four-loop corrections to the electroweak ρ parameter, the precise determination of charm and bottom quark masses and the decoupling constants in QCD. The latter have a close connection to Higgs boson production and decay into gluons and photons which has also been elaborated.

Acknowledgements

This work is supported by the Deutsche Forschungsgemeinschaft in the Sonderforschungsbereich Transregio 9 "Computational Particle Physics".

[1] K. Olive, et al., Review of Particle Physics, Chin.Phys. C38 (2014) 090001. doi:10.1088/1674-1137/38/9/090001.

[2] J. H. Kühn, M. Steinhauser, C. Sturm, Heavy Quark Masses from Sum Rules in Four-Loop Approximation, Nucl.Phys. B778 (2007) 192–215. arXiv:hep-ph/0702103, doi:10.1016/j.nuclphysb.2007.04.036.

[3] K. Chetyrkin, J. Kühn, A. Maier, P. Maierhöfer, P. Marquard, et al., Charm and Bottom Quark Masses: An Update, Phys.Rev. D80 (2009) 074010. arXiv:0907.2110, doi:10.1103/PhysRevD.80.074010.

[4] M. Steinhauser, Leptonic contribution to the effective electromagnetic coupling constant up to three loops, Phys.Lett. B429 (1998) 158–161. arXiv:hep-ph/9803313, doi:10.1016/S0370-2693(98)00503-6.

[5] C. Sturm, Leptonic contributions to the effective electromagnetic coupling at four-loop order in QED, Nucl.Phys. B874 (2013) 698–719. arXiv:1305.0581, doi:10.1016/j.nuclphysb.2013.06.009.

[6] M. Veltman, Limit on Mass Differences in the Weinberg Model, Nucl.Phys. B123 (1977) 89. doi:10.1016/0550-3213(77)90342-X.

[7] R. Barbieri, M. Beccaria, P. Ciafaloni, G. Curci, A. Vicere, Radiative correction effects of a very heavy top, Phys.Lett. B288 (1992) 95–98. arXiv:hep-ph/9205238, doi:10.1016/0370-2693(92)91960-H.

[8] J. Fleischer, O. Tarasov, F. Jegerlehner, Two loop heavy top corrections to the rho parameter: A Simple formula valid for arbitrary Higgs mass, Phys.Lett. B319 (1993) 249–256. doi:10.1016/0370-2693(93)90810-5.

[9] J. van der Bij, K. Chetyrkin, M. Faisst, G. Jikia, T. Seidensticker, Three loop leading top mass contributions to the rho parameter, Phys.Lett. B498 (2001) 156–162. arXiv:hep-ph/0011373, doi:10.1016/S0370-2693(01)00002-8.

[10] M. Faisst, J. H. Kühn, T. Seidensticker, O. Veretin, Three loop top quark contributions to the rho parameter, Nucl.Phys. B665 (2003) 649–662. arXiv:hep-ph/0302275, doi:10.1016/S0550-3213(03)00450-4.

[11] A. Djouadi, C. Verzegnassi, Virtual Very Heavy Top Effects in LEP / SLC Precision Measurements, Phys.Lett. B195 (1987) 265. doi:10.1016/0370-2693(87)91206-8.

[12] A. Djouadi, $O(\alpha\alpha_s)$ Vacuum Polarization Functions of the Standard Model Gauge Bosons, Nuovo Cim. A100 (1988) 357. doi:10.1007/BF02812964.

[13] B. A. Kniehl, J. H. Kühn, R. Stuart, QCD Corrections, Virtual Heavy Quark Effects and Electroweak Precision Measurements, Phys.Lett. B214 (1988) 621. doi:10.1016/0370-2693(88)90132-3.

[14] L. Avdeev, J. Fleischer, S. Mikhailov, O. Tarasov, $O(\alpha\alpha_s^2)$ correction to the electroweak rho parameter, Phys.Lett. B336 (1994) 560–566. arXiv:hep-ph/9406363, doi:10.1016/0370-2693(94)90573-8.

[15] K. Chetyrkin, J. H. Kühn, M. Steinhauser, Corrections of order $O(G_F M_t^2 \alpha_s^2)$ to the ρ parameter, Phys.Lett. B351 (1995) 331–338. arXiv:hep-ph/9502291, doi:10.1016/0370-2693(95)00380-4.

[16] K. Chetyrkin, J. H. Kühn, M. Steinhauser, QCD corrections from top quark to relations between electroweak parameters to order α_s^2, Phys.Rev.Lett. 75 (1995) 3394–3397. arXiv:hep-ph/9504413, doi:10.1103/PhysRevLett.75.3394.

[17] K. Chetyrkin, M. Steinhauser, The relation between the MS-bar and the on-shell quark mass at order α_s^3, Nucl.Phys. B573 (2000) 617–651. arXiv:hep-ph/9911434, doi:10.1016/S0550-3213(99)00784-1.

[18] K. Melnikov, T. v. Ritbergen, The three loop relation between the MS-bar and the pole quark masses, Phys.Lett. B482 (2000) 99–108. arXiv:hep-ph/9912391, doi:10.1016/S0370-2693(00)00507-4.

[19] K. Chetyrkin, M. Faisst, J. H. Kühn, P. Maierhöfer, C. Sturm, Four-Loop QCD Corrections to the Rho Parameter, Phys.Rev.Lett. 97 (2006) 102003. arXiv:hep-ph/0605201, doi:10.1103/PhysRevLett.97.102003.

[20] R. Boughezal, M. Czakon, Single scale tadpoles and $O(G_F m_t^2 \alpha_s^3)$ corrections to the rho parameter, Nucl.Phys. B755 (2006) 221–238. arXiv:hep-ph/0606232, doi:10.1016/j.nuclphysb.2006.08.007.

[21] M. Faisst, P. Maierhöfer, C. Sturm, Standard and epsilon-finite Master Integrals for the rho-Parameter, Nucl.Phys. B766 (2007) 246–268. arXiv:hep-ph/0611244, doi:10.1016/j.nuclphysb.2006.12.014.

[22] Y. Schröder, M. Steinhauser, Four-loop singlet contribution to the rho parameter, Phys.Lett. B622 (2005) 124–130. arXiv:hep-ph/0504055, doi:10.1016/j.physletb.2005.06.085.

[23] I. Allison, et al., High-Precision Charm-Quark Mass from Current-Current Correlators in Lattice and Continuum QCD, Phys.Rev. D78 (2008) 054513. arXiv:0805.2999, doi:10.1103/PhysRevD.78.054513.

[24] C. McNeile, C. Davies, E. Follana, K. Hornbostel, G. Lepage, High-Precision c and b Masses, and QCD Coupling from Current-Current Correlators in Lattice and Continuum QCD, Phys.Rev. D82 (2010) 034512. arXiv:1004.4285, doi:10.1103/PhysRevD.82.034512.

[25] B. Colquhoun, R. Dowdall, C. Davies, K. Hornbostel, G. Lepage, The Υ and Υ' Leptonic Widths, a_μ^b and m_b from full lattice QCD.arXiv:1408.5768.

[26] M. Beneke, A. Maier, J. Piclum, T. Rauh, The bottom-quark mass from non-relativistic sum rules at NNNLO, Nucl.Phys. B891 (2015) 42–72. arXiv:1411.3132, doi:10.1016/j.nuclphysb.2014.12.001.

[27] A. A. Penin, N. Zerf, Bottom Quark Mass from Υ Sum Rules to $O(\alpha_s^3)$, JHEP 1404 (2014) 120. arXiv:1401.7035, doi:10.1007/JHEP04(2014)120.

[28] P. Baikov, K. Chetyrkin, J. H. Kühn, Scalar correlator at $O(\alpha_s^4)$, Higgs decay into b-quarks and bounds on the light quark masses, Phys.Rev.Lett. 96 (2006) 012003. arXiv:hep-ph/0511063, doi:10.1103/PhysRevLett.96.012003.

[29] K. Chetyrkin, J. H. Kühn, M. Steinhauser, RunDec: A Mathematica package for running and decoupling of the strong coupling and quark masses, Comput.Phys.Commun. 133 (2000) 43–65. arXiv:hep-ph/0004189, doi:10.1016/S0010-4655(00)00155-7.

[30] B. Schmidt, M. Steinhauser, CRunDec: a C++ package for running and decoupling of the strong coupling and quark masses, Comput.Phys.Commun. 183 (2012) 1845–1848. arXiv:1201.6149, doi:10.1016/j.cpc.2012.03.023.

[31] K. Chetyrkin, P. Baikov, J. Kühn, Towards QCD running in 5 loops: quark mass anomalous dimension, PoS RADCOR2013 (2013) 056. arXiv:1402.6606.

[32] P. Baikov, K. Chetyrkin, J. Kühn, Quark Mass and Field Anomalous Dimensions to $O(\alpha_s^5)$, JHEP 1410 (2014) 76. arXiv:1402.6611, doi:10.1007/JHEP10(2014)076.

[33] V. Novikov, L. Okun, M. A. Shifman, A. Vainshtein, M. Voloshin, et al., Charmonium and Gluons: Basic Experimental Facts and Theoretical Introduction, Phys.Rept. 41 (1978) 1–133. doi:10.1016/0370-1573(78)90120-5.

[34] K. Chetyrkin, J. H. Kühn, M. Steinhauser, Heavy quark vacuum polarization to three loops, Phys.Lett. B371 (1996) 93–98. arXiv:hep-ph/9511430, doi:10.1016/0370-2693(95)01593-0.

[35] K. G. Chetyrkin, J. H. Kühn, M. Steinhauser, Three-loop polarization function and $O(\alpha_s^2)$ corrections to the production of heavy quarks, Nucl. Phys. B482 (1996) 213–240. arXiv:hep-ph/9606230, doi:10.1016/S0550-3213(96)00534-2.

[36] K. G. Chetyrkin, J. H. Kühn, M. Steinhauser, Heavy quark current correlators to $O(\alpha_s^2)$, Nucl. Phys. B505 (1997) 40–64. arXiv:hep-ph/9705254, doi:10.1016/S0550-3213(97)00481-1.

[37] R. Boughezal, M. Czakon, T. Schutzmeier, Four-loop tadpoles: Applications in QCD, Nucl. Phys. Proc. Suppl. 160 (2006) 160–164. arXiv:hep-ph/0607141.

[38] A. Maier, P. Maierhöfer, P. Marquard, Higher Moments of Heavy Quark Correlators in the Low Energy Limit at $O(\alpha_s^2)$, Nucl. Phys. B797 (2008) 218–242. arXiv:0711.2636, doi:10.1016/j.nuclphysb.2007.12.035.

[39] K. Chetyrkin, J. H. Kuhn, P. Mastrolia, C. Sturm, Heavy-quark vacuum polarization: First two moments of the $O(\alpha_s^3 n_f^2)$ contribution, Eur.Phys.J. C40 (2005) 361–366. arXiv:hep-ph/0412055, doi:10.1140/epjc/s2005-02151-y.

[40] S. Laporta, High precision calculation of multiloop Feynman integrals by difference equations, Int.J.Mod.Phys. A15 (2000) 5087–5159. arXiv:hep-ph/0102033, doi:10.1016/S0217-751X(00)00215-7.

[41] K. Chetyrkin, J. H. Kühn, C. Sturm, Four-loop moments of the heavy quark vacuum polarization function in perturbative QCD, Eur.Phys.J. C48 (2006) 107–110. arXiv:hep-ph/0604234, doi:10.1140/epjc/s2006-02610-y.

[42] R. Boughezal, M. Czakon, T. Schutzmeier, Charm and bottom quark masses from perturbative QCD, Phys. Rev. D74 (2006) 074006. arXiv:hep-ph/0605023.

[43] A. Maier, P. Maierhöfer, P. Marquard, The Second physical moment of the heavy quark vector correlator at $O(\alpha_s^3)$, Phys.Lett. B669 (2008) 88–91. arXiv:0806.3405, doi:10.1016/j.physletb.2008.09.041.

[44] A. Maier, P. Maierhöfer, P. Marquard, A. Smirnov, Low energy moments of heavy quark current correlators at four loops, Nucl.Phys. B824 (2010) 1–18. arXiv:0907.2117, doi:10.1016/j.nuclphysb.2009.08.011.

[45] S. Laporta, High precision epsilon expansions of massive four loop vacuum bubbles, Phys.Lett. B549 (2002) 115–122. arXiv:hep-ph/0210336, doi:10.1016/S0370-2693(02)02910-6.

[46] Y. Schroder, A. Vuorinen, High-precision epsilon expansions of single-mass-scale four-loop vacuum bubbles, JHEP 0506 (2005) 051. arXiv:hep-ph/0503209, doi:10.1088/1126-6708/2005/06/051.

[47] K. Chetyrkin, M. Faisst, C. Sturm, M. Tentyukov, ε-finite basis of master integrals for the integration-by-parts method, Nucl.Phys. B742 (2006) 208–229. arXiv:hep-ph/0601165, doi:10.1016/j.nuclphysb.2006.02.030.

[48] R. Lee, I. Terekhov, Application of the DRA method to the calculation of the four-loop QED-type tadpoles, JHEP 1101 (2011) 068. arXiv:1010.6117, doi:10.1007/JHEP01(2011)068.

[49] A. H. Hoang, V. Mateu, S. Mohammad Zebarjad, Heavy Quark Vacuum Polarization Function at $O(\alpha_s^2)$ and $O(\alpha_s^3)$, Nucl.Phys. B813 (2009) 349–369. arXiv:0807.4173, doi:10.1016/j.nuclphysb.2008.12.005.

[50] Y. Kiyo, A. Maier, P. Maierhöfer, P. Marquard, Reconstruction of heavy quark current correlators at $O(\alpha_s^3)$, Nucl.Phys.

B823 (2009) 269–287. arXiv:0907.2120, doi:10.1016/j.nuclphysb.2009.08.010.

[51] D. Greynat, S. Peris, Resummation of Threshold, Low- and High-Energy Expansions for Heavy-Quark Correlators, Phys.Rev. D82 (2010) 034030. arXiv:1006.0643, doi:10.1103/PhysRevD.82.119907,10.1103/PhysRevD.82.034030.

[52] C. Sturm, Moments of Heavy Quark Current Correlators at Four-Loop Order in Perturbative QCD, JHEP 0809 (2008) 075. arXiv:0805.3358, doi:10.1088/1126-6708/2008/09/075.

[53] A. Grozin, C. Sturm, Correlator of heavy-quark currents at small q^2 in the large-beta(0) limit, Eur.Phys.J. C40 (2005) 157–164. arXiv:hep-ph/0412040, doi:10.1140/epjc/s2005-02124-2.

[54] J. Bai, et al., Measurements of the cross-section for $e^+e^- \to$ hadrons at center-of-mass energies from 2 GeV to 5 GeV, Phys.Rev.Lett. 88 (2002) 101802. arXiv:hep-ex/0102003, doi:10.1103/PhysRevLett.88.101802.

[55] M. Ablikim, J. Bai, Y. Ban, J. Bian, X. Cai, et al., Measurements of the continuum R_{uds} and R values in e^+e^- annihilation in the energy region between 3.650 and 3.872 GeV, Phys.Rev.Lett. 97 (2006) 262001. arXiv:hep-ex/0612054, doi:10.1103/PhysRevLett.97.262001.

[56] A. Blinov, V. Blinov, A. Bondar, A. Bukin, V. Groshev, et al., The measurement of R in e^+e^- annihilation at center-of-mass energies between 7.2 GeV and 10.34 GeV, Z.Phys. C70 (1996) 31–38. doi:10.1007/s002880050077.

[57] R. Ammar, et al., A measurement of the total cross-section for $e^+e^- \to$ hadrons at $s^{(1/2)} = 10.52$ GeV, Phys.Rev. D57 (1998) 1350–1358. arXiv:hep-ex/9707018, doi:10.1103/PhysRevD.57.1350.

[58] J. H. Kühn, M. Steinhauser, Determination of α_s and heavy quark masses from recent measurements of R(s), Nucl.Phys. B619 (2001) 588–602. arXiv:hep-ph/0109084, doi:10.1016/S0550-3213(01)00499-0.

[59] J. Rolf, S. Sint, A Precise determination of the charm quark's mass in quenched QCD, JHEP 0212 (2002) 007. arXiv:hep-ph/0209255, doi:10.1088/1126-6708/2002/12/007.

[60] A. Signer, The Charm quark mass from non-relativistic sum rules, Phys.Lett. B672 (2009) 333–338. arXiv:0810.1152, doi:10.1016/j.physletb.2009.01.028.

[61] K. Chetyrkin, J. Kühn, A. Maier, P. Maierhofer, P. Marquard, et al., Precise Charm- and Bottom-Quark Masses: Theoretical and Experimental Uncertainties, Theor.Math.Phys. 170 (2012) 217–228. arXiv:1010.6157, doi:10.1007/s11232-012-0024-7.

[62] S. Bodenstein, J. Bordes, C. Dominguez, J. Penarrocha, K. Schilcher, QCD sum rule determination of the charm-quark mass, Phys.Rev. D83 (2011) 074014. arXiv:1102.3835, doi:10.1103/PhysRevD.83.074014.

[63] J. Heitger, G. M. von Hippel, S. Schaefer, F. Virotta, Charm quark mass and D-meson decay constants from two-flavour lattice QCD, PoS LATTICE2013 (2014) 475. arXiv:1312.7693.

[64] N. Carrasco, et al., Up, down, strange and charm quark masses with $N_f = 2+1+1$ twisted mass lattice QCD, Nucl.Phys. B887 (2014) 19–68. arXiv:1403.4504, doi:10.1016/j.nuclphysb.2014.07.025.

[65] B. Chakraborty, C. Davies, G. Donald, R. Dowdall, B. Galloway, et al., High-precision quark masses and QCD coupling from $n_f = 4$ lattice QCD.arXiv:1408.4169.

[66] B. Dehnadi, A. H. Hoang, V. Mateu, Charm and Bottom Masses from Sum Rules with a Convergence Test.arXiv:1411.5597.

[67] W. Yao, et al., Review of Particle Physics, J.Phys. G33 (2006) 1–1232. doi:10.1088/0954-3899/33/1/001.

[68] B. Aubert, et al., Measurement of the $e^+e^- \to b\bar{b}$ cross section between $\sqrt{s}$ = 10.54-GeV and 11.20-GeV, Phys.Rev.Lett. 102 (2009) 012001. arXiv:0809.4120, doi:10.1103/PhysRevLett.102.012001.

[69] D. Besson, et al., Observation of new structure in the e^+e^- annihilation cross-section above B anti-B threshold, Phys.Rev.Lett. 54 (1985) 381. doi:10.1103/PhysRevLett.54.381.

[70] A. Pineda, A. Signer, Renormalization group improved sum rule analysis for the bottom quark mass, Phys.Rev. D73 (2006) 111501. arXiv:hep-ph/0601185, doi:10.1103/PhysRevD.73.111501.

[71] S. Bodenstein, J. Bordes, C. Dominguez, J. Penarrocha, K. Schilcher, Bottom-quark mass from finite energy QCD sum rules, Phys.Rev. D85 (2012) 034003. arXiv:1111.5742, doi:10.1103/PhysRevD.85.034003.

[72] C. Ayala, G. Cveti, A. Pineda, The bottom quark mass from the $\Upsilon(1S)$ system at NNNLO, JHEP 1409 (2014) 045. arXiv:1407.2128, doi:10.1007/JHEP09(2014)045.

[73] K. Chetyrkin, J. H. Kühn, C. Sturm, QCD decoupling at four loops, Nucl.Phys. B744 (2006) 121–135. arXiv:hep-ph/0512060, doi:10.1016/j.nuclphysb.2006.03.020.

[74] Y. Schröder, M. Steinhauser, Four-loop decoupling relations for the strong coupling, JHEP 0601 (2006) 051. arXiv:hep-ph/0512058, doi:10.1088/1126-6708/2006/01/051.

[75] K. Chetyrkin, B. A. Kniehl, M. Steinhauser, Decoupling relations to $O(\alpha_s^3)$ and their connection to low-energy theorems, Nucl.Phys. B510 (1998) 61–87. arXiv:hep-ph/9708255, doi:10.1016/S0550-3213(97)00649-4.

[76] C. Sturm, Higher order QCD results for the fermionic contributions of the Higgs-boson decay into two photons and the decoupling function for the $\overline{\rm MS}$ renormalized fine-structure constant, Eur.Phys.J. C74 (8) (2014) 2978. arXiv:1404.3433, doi:10.1140/epjc/s10052-014-2978-0.

[77] M. Steinhauser, Corrections of $O(\alpha_s^2)$ to the decay of an intermediate mass Higgs boson into two photons.arXiv:hep-ph/9612395.

[78] P. Maierhöfer, P. Marquard, Complete three-loop QCD corrections to the decay $H \to \gamma\gamma$, Phys.Lett. B721 (2013) 131–135. arXiv:1212.6233, doi:10.1016/j.physletb.2013.02.040.

[79] D. Besson, et al., Measurement of the Total Hadronic Cross Section in e^+e^- Annihilations below 10.56-GeV, Phys.Rev. D76 (2007) 072008. arXiv:0706.2813, doi:10.1103/PhysRevD.76.072008.